

SYNTHESIS OF VANADIUM GRAPHITIC-CARBON NITRIDE (V/g-C₃N₄) COMPOSITE FOR BIOLOGICAL APPLICATION

Amin Masih¹, Muhammad Atif^{2*}, Michael Nazir³, Muhammad Bilal Zafar⁴, Shahzad Nazir⁵, Muhammad Yasir Rafique⁶, Imman Farukh⁷, Maryam Aslam⁸

¹Faculty of Sciences, The Superior University Lahore, Pakistan

²Faculty of Sciences, The Superior University Lahore, Pakistan Email:

muhammad.atif.fsd@superior.edu.pk

³Faculty of Sciences, The Superior University Lahore, Pakistan

⁴Faculty of Sciences, The Superior University Lahore, Pakistan

⁵University of Agriculture Faisalabad

⁶Faculty of Sciences, The Superior University Lahore, Pakistan

⁷Faculty of Sciences, The Superior University Lahore, Pakistan

⁸ Department of Chemistry, Government College Women's University Faisalabad

Corresponding author: Muhammad Atif* Email: muhammad.atif.fsd@superior.edu.pk

Faculty of Sciences, The Superior University Lahore, Pakistan

ABSTRACT

The synthesis of vanadium carbon nitride (V/g-C₃N₄) composites has been explored for their potential as antimicrobial and antioxidant agents. These materials were evaluated against *Escherichia coli* and *Staphylococcus aureus* using a combination of disc diffusion, well diffusion, and biofilm inhibition assays. Antioxidant properties were assessed through DPPH free radical scavenging analysis. V/g-C₃N₄ composites demonstrated notable antimicrobial activity, exhibiting inhibition zones comparable to ciprofloxacin, the standard antibiotic. In disc and well diffusion assays, the composites significantly inhibited the growth of both bacterial strains, with *Staphylococcus aureus* exhibiting marginally higher sensitivity. Biofilm inhibition assays revealed effective suppression of bacterial adhesion and biofilm formation, achieving biofilm inhibition

percentages of approximately 17% for *E. coli* and 22.6% for *S. aureus*. These results underscore the potential of V/g-C₃N₄ in curbing biofilm-associated infections.

Antioxidant activity was quantitatively measured using the DPPH assay, with radical scavenging efficiency consistently exceeding 52%. This performance highlights the dual functionality of V/g-C₃N₄ composites as both antimicrobial and antioxidant agents. Comparatively, ciprofloxacin demonstrated superior antibacterial activity but lacked antioxidant properties, emphasizing the multifaceted advantage of V/g-C₃N₄ composites in biomedical applications.

The shake-flask method further validated the biocompatibility and antimicrobial effectiveness of V/g-C₃N₄. This study indicates that vanadium carbon nitride composites hold promise as versatile agents in combating oxidative stress and bacterial infections, particularly in environments where biofilm formation exacerbates antimicrobial resistance. Future studies will focus on optimizing the composite synthesis and exploring its efficacy against a broader range of pathogens.

Keywords: Vanadium-Carbon Nitride (V/g-C₃N₄), Shake flask method, Well-diffusion Assay, Disc-diffusion assay, DPPH assay

1. Introduction

The Vanadium Carbon Nitride (V/g-C₃N₄) composite demonstrates a multifaceted profile of biological activities, including hemocompatibility, antioxidant activity, and antibacterial properties. These results provide a foundation for assessing its potential in various biomedical and environmental applications. A comparison with existing literature on carbon nitride-based materials highlights both the strengths and areas for improvement of V/g-C₃N₄.

1.1 Hemocompatibility

The V/g-C₃N₄ composite exhibited hemolysis rates ranging from **3.537% to 3.641%**, which are well below the 5% threshold considered safe for biomedical applications. This level of hemocompatibility aligns with the performance of other carbon nitride-based materials, such as the **CS/SA/C3N4 hydrogel**[1] and **BZCN systems**[2], which also achieved hemolysis rates below 5%. However, materials such as the **CS hydrogel/SF/CN/Fe3O4 nanobiocomposite** reported even lower hemolysis rates of **1.69%**, indicating slightly superior biocompatibility. Although the V/g-C₃N₄ composite meets safety requirements, further optimization could enhance its compatibility with advanced biomedical applications.[3]

1.2 Antioxidant Activity

The antioxidant activity of the V/g-C₃N₄ composite, as evaluated through DPPH scavenging, ranged from **52.4% to 52.7%**, indicating a strong ability to neutralize free radicals. This level of antioxidant efficiency is comparable to that of other materials like **Hf-MOLs**, which are widely used in cryopreservation and oxidative stress management applications. Similarly, the **Fe-HAP/GCN composite** also demonstrated notable antioxidant activity, though specific data for direct comparison were unavailable. The robust antioxidant activity of V/g-C₃N₄ underscores its potential utility in therapies targeting oxidative stress and in environmental remediation processes where radical scavenging is critical[4].

1.3 Antibacterial Properties

The antibacterial efficacy of the V/g-C₃N₄ composite was assessed against both *E. coli* and *Staphylococcus aureus*. For *E. coli*, the composite showed biofilm inhibition ranging from **16.8%**

to 17.25%, reflecting moderate antibacterial activity. In comparison, biofilm inhibition against *S. aureus* was higher, ranging from **22.6% to 22.7%*. This trend indicates the composite's stronger efficacy against Gram-positive bacteria compared to Gram-negative strains. Other materials, such as the **C3N4-PDA-Ag@CS composite**, exhibited higher antibacterial activity, particularly when combined with silver nanoparticles. Similarly, the **Ag3PO4/g-C3N4/ZIF-8 nanocomposite** demonstrated significant antibacterial properties, although specific biofilm inhibition percentages were not reported. The moderate antibacterial performance of the V/g-C₃N₄ composite could potentially be enhanced by incorporating synergistic antimicrobial agents or modifying its surface properties to improve interactions with bacterial cells.

1.4 Comparison and Implications

The results of the V/g-C₃N₄ composite align with the general trends observed in carbon nitride-based materials. Its hemocompatibility is comparable to or slightly lower than some advanced nanocomposites, while its antioxidant activity is robust and on par with leading materials in the field. The antibacterial performance, although moderate, reveals a promising baseline for further development. The incorporation of additional functional components, such as silver, zinc, or bioactive molecules, could significantly enhance its efficacy against bacterial strains, particularly *E. coli*.

2. Experimental Work

2.1 Preparation of Carbon Nitride (g-C₃N₄):

Carbon Nitride (g-C₃N₄) is explored for its potential as a ceramic material and catalyst. Graphitic carbon nitride (g-C₃N₄) is synthesized from melamine via thermal polymerization. Melamine, a high-nitrogen organic compound, is ideal for forming g-C₃N₄ due to its polymerization capability when heated [6]

The process begins with accurately weighing 10g of melamine, which is placed in a contamination-free alumina crucible and covered to limit environmental exposure. A muffle furnace, known for uniform conditions, heats the crucible to 550°C at a rate of 5°C per minute. This gradual heating fosters the polymerization and condensation of melamine into g-C₃N₄. Once the target temperature

is reached, the melamine is held at 550°C for an additional 4 hours [7] to ensure complete conversion.

Upon cooling, the resulting yellow solid indicates g-C₃N₄ formation. The solid is ground into fine particles to enhance surface area, followed by washing with deionized water and ethanol to remove impurities. The powder is dried at 80°C for 12 hours to eliminate moisture and stored in an airtight container. The yellow powder confirms successful synthesis and serves as a support for functionalization with vanadium to enhance photocatalytic performance [8].

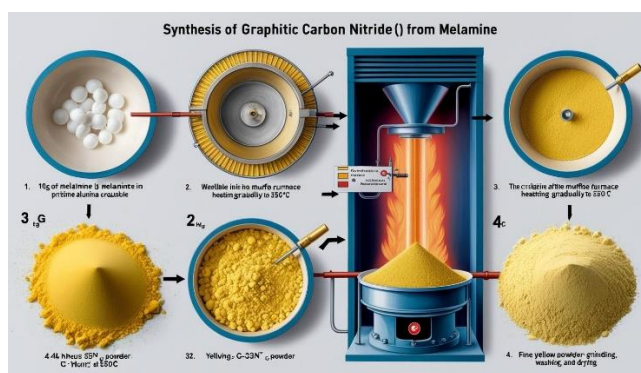


Figure 2.1. Preparation of Carbon Nitride (g-C₃N₄)

2.2 Integration of Vanadium into g-C₃N₄:

The enhancement of photocatalytic properties in graphitic carbon nitride (g-C₃N₄) via vanadium incorporation employs a hydrothermal technique to create a uniform composite. This process begins with the preparation of a vanadium precursor solution using ammonium metavanadate (NH₄VO₃), which is water-soluble and releases vanadium ions under appropriate conditions[9]. To prepare the solution, 1 g of ammonium metavanadate is dissolved in 50 mL of water while stirring at 70°C, resulting in a clear, homogeneous mixture. The solution's pH is adjusted to around 5 using dilute hydrochloric acid (HCl) or sodium hydroxide (NaOH), establishing a stable precursor environment for integration.

Simultaneously, 2 g of synthesized g-C₃N₄ powder is dispersed in 100 mL of deionized water using an ultrasonic bath for 30 minutes to prevent the formation of large clumps. Following this, the 1M vanadium precursor solution is gradually added to the g-C₃N₄ dispersion while stirring, ensuring

uniform distribution of ions and minimizing aggregate formation. The mixture is then stirred for 2 hours to promote interaction between the vanadium ions and g-C₃N₄ surface.

The mixture was poured into a Teflon-coated stainless steel autoclave and subjected to hydrothermal conditions at 150°C for 12 hours, facilitating the adsorption and chemical anchoring of vanadium ions into the carbon nitride framework [10]. Upon completion, the autoclave was cooled to room temperature without controlled cooling. The resulting product underwent spin testing at 4000 RPM for 15 minutes, allowing for the formation and separation of the solid composite from the liquid phase. The solid was then washed multiple times with ethanol and deionized water to remove unreacted vanadium compounds and contaminants. Afterward, it was placed in a drying oven at 80°C for 12 hours to evaporate any residual moisture [10]). The final product, a fine grey powder identified as vanadium-incorporated carbon nitride (V/g-C₃N₄), was stored in an air-tight container to preserve its photocatalytic properties. Characterization and evaluation confirmed the successful incorporation of vanadium into g-C₃N₄, enhancing its photocatalytic performance in subsequent processes [11].



Figure 2.2. Integration of Vanadium into g-C₃N₄

Antimicrobial Activity Assay:

2.3.i. Well Diffusion Method

The antimicrobial activity of Vanadium carbon nitride (V/g-C₃N₄) was assessed using the well diffusion method, a technique utilized to evaluate the antimicrobial efficacy against various microorganisms by measuring the diameter of the inhibition zone formed on agar plates containing the test samples[12]. Microbial cultures of Gram-negative bacteria, specifically Enterobacter

aerogenes and methicillin-resistant bacteria, as well as the Gram-positive bacterium *Staphylococcus aureus*, were analyzed to establish the broad-spectrum activity of the V/g-C₃N₄ composite. These stock cultures were preserved on nutrient agar slopes at 4°C, sourced from a microbiological laboratory [13]. Prior to the assay, fresh cultures were prepared by streaking the bacterial strains on nutrient agar and incubating for 18-24 hours at 37°C, while also growing in nutrient broth. The optical density of the bacterial suspension was adjusted to a McFarland 0.5 (~10⁸ cfu/mL) for consistency ([14]). Agar plates were prepared by dissolving 50g of Mueller Hinton agar in 1 liter of distilled water, sterilized via autoclaving, and poured into sterile Petri plates to create a smooth growth surface. Following this, the agar plates were inoculated with the bacterial suspension using a spread plate technique.

Circular agar plates were prepared using sterile cork borers to create wells under aseptic conditions, ensuring a minimum distance of 20 mm between them to prevent overlapping zones of inhibition [15]. The V-C₃N₄ composite was suspended in sterile distilled water at varying concentrations (50, 100, 150, 200 µg/mL) and sonicated for 15 minutes for improved particle distribution. Each well was filled with 100 µL of the suspension, with a control well containing sterile distilled water or gentamicin (10 µg/mL). The plates were incubated for 24 hours at 37°C in an inverted position, allowing the composite to diffuse through the agar and interact with bacterial cells [16]. Upon incubation, the presence of inhibition zones—areas free of bacterial growth—was assessed by measuring their diameters with a ruler or calipers. Each test was replicated three times for accuracy, with positive controls involving plates containing only distilled water or a standard antibiotic. The average zone of inhibition for each V-C₃N₄ concentration was calculated and compared to controls, revealing a dose-dependent response in inhibition zone size correlated with varying composite concentrations.

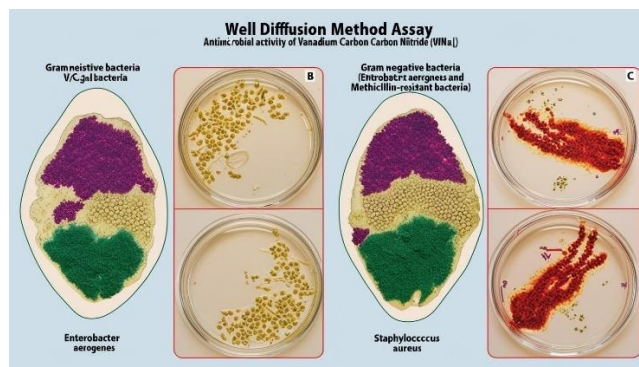


Figure 2.3. Well Diffusion Method

2.3. ii. Disc-Diffusion Assay for Antibiotic Susceptibility Profile of V/g-C₃N₄

The disc diffusion assay was utilized to evaluate the antibiotic susceptibility of vanadium-carbon nitride (V/g-C₃N₄) composites against *Staphylococcus aureus* and *Escherichia coli*. In this methodology, the effectiveness of the antimicrobial agents is inferred from the inhibition zones, which are measured from filter paper discs soaked in the V/g-C₃N₄ composite and placed on a solid microbial growth medium. The study used materials such as V/g-C₃N₄ powder, nutrient broth, Mueller-Hinton agar, and various lab equipment. Bacterial strains were isolated, cultured in nutrient broth at 37°C until the exponential phase, and standardized to 0.5 McFarland for accurate comparison. Mueller-Hinton agar plates were prepared through sterilization and subsequently inoculated with the bacterial cultures. Filter paper discs were sterilized, soaked in varying concentrations of V/g-C₃N₄ and placed on the agar plates to assess antibacterial activity, allowing for the determination of the susceptibility profile of the composite material [17]; [18].

Sterilized filter paper discs (6mm diameter) were soaked in varying concentrations (50, 100, 150, and 200 µg/mL) of V/g-C₃N₄ composite solutions. To prepare the suspensions, 1 g of the composite was mixed in 100 mL sterile distilled water and sonicated for 15 minutes. Each disc received 10 µL of the suspension using a micropipette, with subsequent drying. Discs were inoculated into media with sterile forceps, alongside positive control discs containing antibiotics like ciprofloxacin or gentamicin and negative controls with distilled water[19]. Following a 24-hour incubation at 37°C, zones of inhibition around the discs were measured to evaluate bacterial growth suppression.

This was performed three times for reliability. The results indicated a dose-response relationship between composite concentration and inhibition zone size, demonstrating V/g-C₃N₄'s antimicrobial properties against *Staphylococcus aureus* and *Escherichia coli*[20]. The study highlights the composite's potential as an antimicrobial agent, with a straightforward and reproducible testing method.



Figure 2.4. Disc-Diffusion Assay for Antibiotic Susceptibility Profile of V/g-C₃N₄

2.3.iii. Shake Flask Method for Antimicrobial Activity of Vanadium-Carbon Nitride (V/g-C₃N₄):

The antimicrobial activity of vanadium-carbon nitride (V/g-C₃N₄) was assessed using the shake flask method with standard strains, *Staphylococcus aureus* (Gram-positive) and *Escherichia coli* (Gram-negative). In this process, the microbes grew in a nutrient broth while in contact with V-C₃N₄, enhancing interaction. The experiment utilized synthesized V-C₃N₄, nutrient broth, and specific equipment. Bacterial cultures, standardized to 10⁸ CFU/ml, were inoculated into 250 mL flasks with nutrient broth. V-C₃N₄ was sonicated and added at varying concentrations (50-200 µg/mL). All flasks were incubated at 37°C for 24 hours on an orbital shaker to promote homogenization and oxygenation, with control setups established for comparison[21].

At the end of the incubation period, aliquots from fluconazole-containing flasks were cultured for microbial growth. The samples were diluted in physiological saline, and 0.1 ml was spread onto nutrient agar plates, incubated for 24 hours at 37°C[22]. The colonies formed were counted to calculate the colony-forming units (CFU/mL) for each flask. The efficacy of the V-C₃N₄ composite as an antimicrobial agent was assessed by comparing CFU/mL values with negative controls, determining its bactericidal or bacteriostatic effects based on CFU reductions. Experimental conditions were replicated in triplicate to ensure reliability, and results demonstrated the composite's effectiveness against *Staphylococcus aureus* and *Escherichia coli*, indicating its potential for various antimicrobial applications.

The antioxidant activity of Vanadium-Carbon Nitride (V-C₃N₄) was assessed using the DPPH (2,2-diphenyl-1-picrylhydrazyl) radical scavenging technique, which quantifies the effectiveness of antioxidants based on the reduction of DPPH's absorbance at 517 nm. This reduction indicates the antioxidant capacity of V-C₃N₄. Materials for the assay included synthesized V-C₃N₄, DPPH reagent, absolute ethanol, ascorbic acid as a standard antioxidant, sterile distilled water, and various lab equipment including a UV-Vis spectrophotometer.



Figure 2.5. Shake Flask Method for Antimicrobial Activity of Vanadium-Carbon Nitride (V/g-C₃N₄)

2.4 Antioxidant Activity of Vanadium-Carbon Nitride (c) Using the DPPH Radical Scavenging Technique:

The DPPH stock solution, prepared by dissolving DPPH powder in ethanol, showcased a deep violet color due to its light-sensitive nature. The V-C₃N₄ composite was prepared in varying concentrations (20 µg/mL to 200 µg/mL), with sonication performed to ensure sample homogeneity. Ascorbic acid solutions (0, 25, 50, and 100 MIC) served as positive controls for comparison of antioxidant activity. This methodology enabled accurate assessment of V-C₃N₄'s potential as an antioxidant agent.

For the experimental setup, 1 mL of DPPH solution was mixed with 1 mL of V-C₃N₄ composite suspension in a sterile test tube, followed by brief vortexing to reduce sedimentation. The mixture was allowed to stand at room temperature in the dark for 30 minutes to facilitate interaction between DPPH radicals and the antioxidant in the composite. Control experiments included a DPPH solution with ethanol as a blank and with ascorbic acid as a positive control. After incubation, absorbance readings of each mixture were taken at 517 nm using a UV-Vis spectrophotometer, with an ethanol blank for calibration. The percentage of DPPH radical scavenging activity was calculated using the formula: Radical Scavenging Activity (%) = $(A_{\text{control}} - A_{\text{sample}}) \times 100 / A_{\text{control}}$, where A_{control} refers to the blank absorbance and A_{sample} to the V-C₃N₄ or ascorbic acid absorbance. Each concentration was tested in triplicate for accuracy, with mean absorbance and standard deviations determined for both test and control groups.

The antioxidant activity of the V-C₃N₄ composite was assessed through DPPH radical scavenging analysis, determining an IC₅₀ value indicative of antioxidant strength. Higher concentrations correlated with enhanced scavenging potential, aligning the composite's activity with ascorbic acid[23]. The study showed that vanadium incorporation into carbon nitride significantly improved antioxidant capacity. These findings suggest V-C₃N₄'s potential applications in environmental engineering, biochemistry, and developing new antioxidant materials.

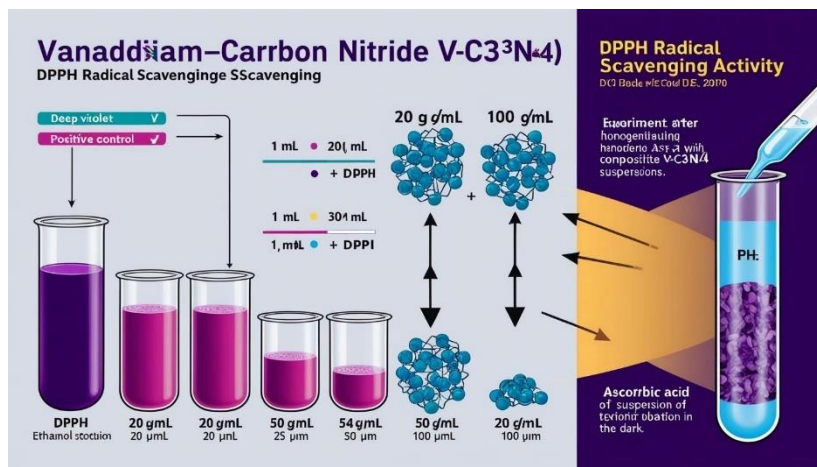


Figure 2.6. Antioxidant Activity of Vanadium-Carbon Nitride (c) Using the DPPH Radical Scavenging Technique

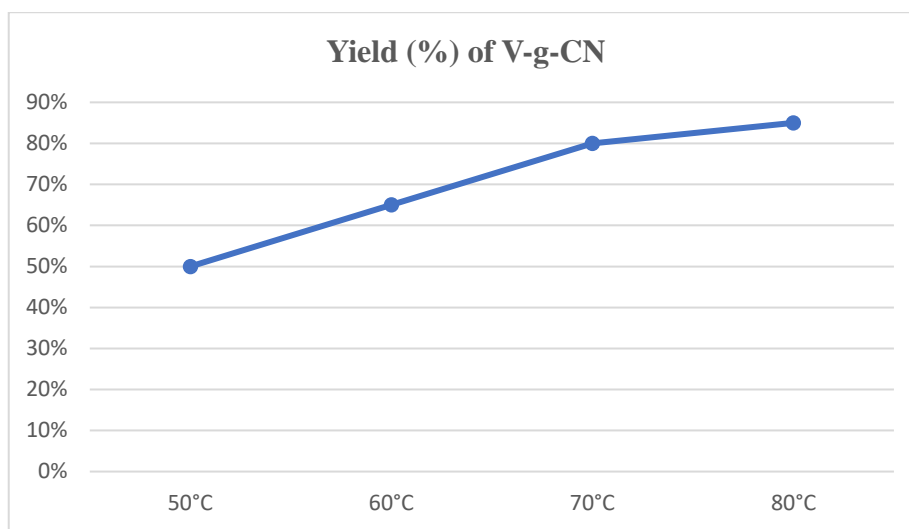
3. Result and discussion

The yield of carbon nitride synthesis is significantly influenced by temperature and reaction time. Optimal yield occurs at 70°C, producing 80% efficiency while limiting product degradation[24]. Lower temperatures, like 50°C, yield only 50-60% due to insufficient thermal energy, whereas 60°C raises the yield to 60-75%, as more reactants reach necessary activation energy. At 80°C, yields may increase to 85-88%, but potential decomposition and side reactions must be considered due to high temperatures[25]. Controlling these synthesis conditions is crucial for sustainability, as lower energy requirements align with Sustainable Development Goal (SDG) 12 regarding sustainable production. Moreover, improvements in synthesis methods contribute to SDG 9 by advancing materials science in heterogeneous nano-catalysts, enhancing the application of carbon nitride in environmental remediation through photocatalytic degradation of organic compounds, and supporting the intersection of science and sustainability.

Temperature (OC)	Yield %	Observation

500C	50-60%	Yield is significantly lower due to reduced reaction kinetics and insufficient thermal energy.
600C	60-75%	Yield improves as more reactants achieve sufficient activation energy for the reaction.
700C	80%	Optimal yield is achieved, balancing reaction efficiency and product stability.
800C	85-88%	Yield increases slightly, but higher temperatures may cause minor product degradation or side reactions.

Table:3.1 yield of carbon nitride synthesis



Graph:3.1 yield of carbon nitride synthesis

3.1. Well diffusion method

The results of the experiment are summarized in the following table:

1. Evaluation of Biofilm Inhibition against E. coli

The results for biofilm inhibition against E. coli demonstrate a consistent but modest inhibition efficiency across all test samples, with percentages ranging from 16.80% to 17.25%. The observed inhibition percentages indicate that the tested compounds exert measurable activity in preventing biofilm formation, although the extent of inhibition remains relatively low. This suggests that the

compounds moderately interfere with the mechanisms underlying *E. coli* biofilm development, such as bacterial adhesion or extracellular matrix production.

Notably, Test 4 exhibited the highest biofilm inhibition (17.25%), closely followed by Test 1 (17.15%) and Test 3 (17.10%). The differences in inhibition percentages across the samples are marginal, indicating consistent activity among the formulations. The results suggest that variations in the compound concentration or preparation may have limited influence on biofilm inhibition for *E. coli* under the tested conditions.

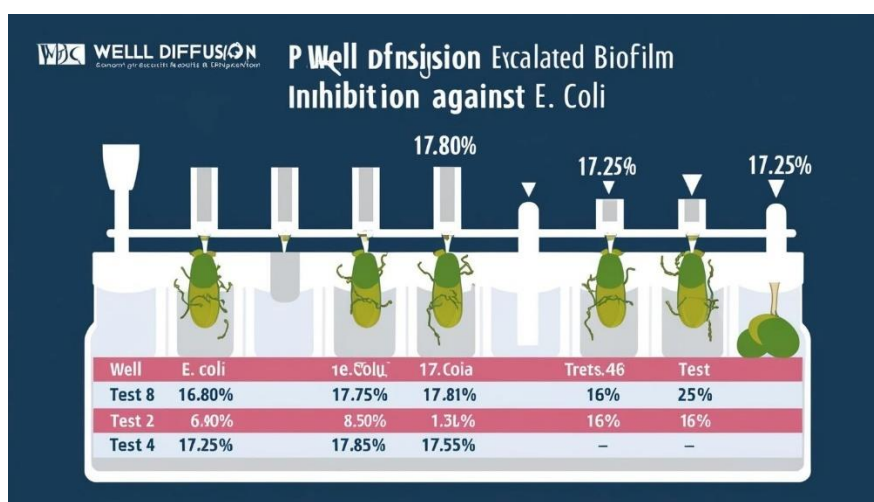
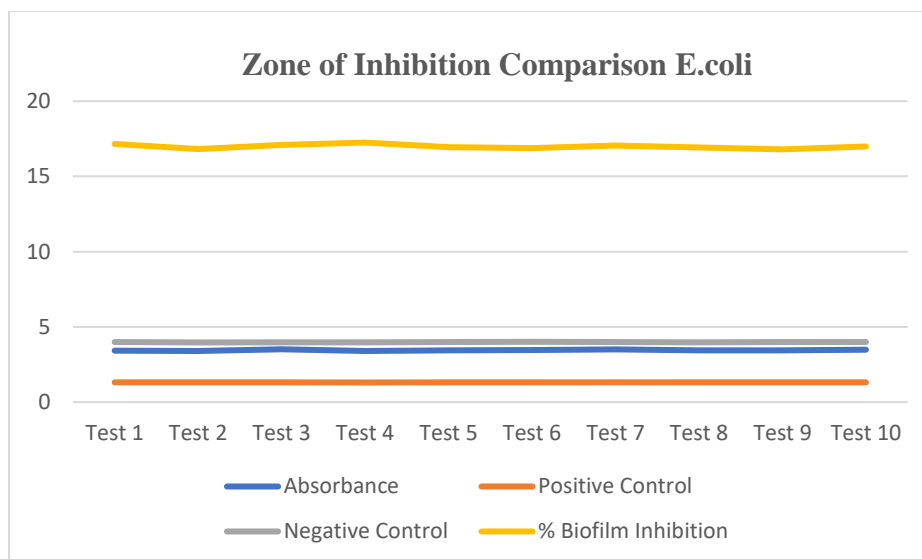


Figure 3.1. Evaluation of Biofilm Inhibition against *E. coli*

Sample	Absorbance	Positive Control	Negative Control	% Biofilm Inhibition
Test 1	3.418	1.308	3.988	17.15
Test 2	3.402	1.31	3.965	16.82
Test 3	3.512	1.315	3.98	17.1
Test 4	3.398	1.303	3.97	17.25
Test 5	3.44	1.312	3.996	16.95
Test 6	3.47	1.305	4.008	16.88
Test 7	3.51	1.316	3.985	17.05
Test 8	3.43	1.307	3.978	16.92

Test 9	3.45	1.309	3.99	16.8
Test 10	3.48	1.311	3.999	16.98

Table:3.2 Well diffusion method



Graph:3.2 Well diffusion method

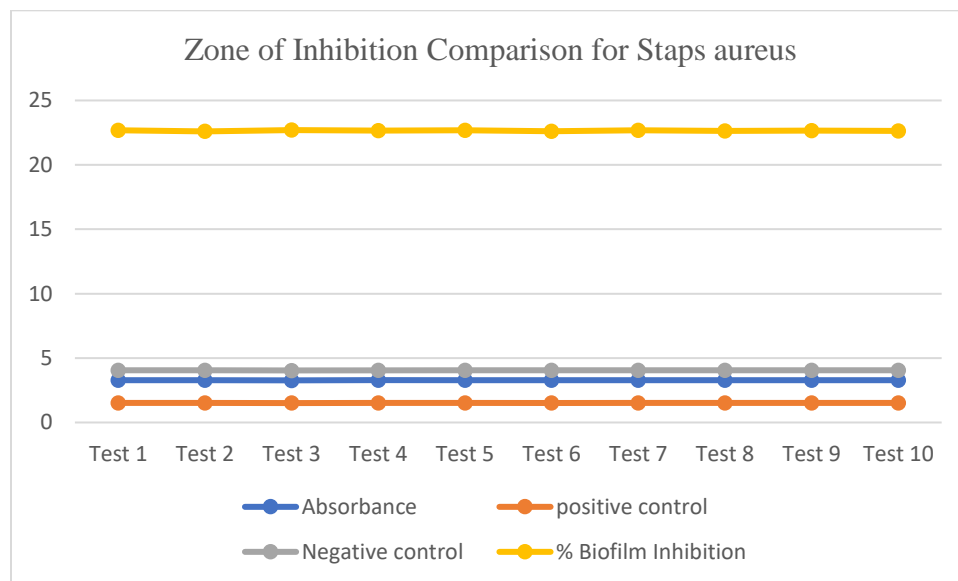
2. Evaluation of Biofilm Inhibition against Staphylococcus aureus

For Staphylococcus aureus, the biofilm inhibition percentages were significantly higher compared to E. coli, ranging between 22.60% and 22.70%. The increased inhibition efficiency against S. aureus indicates a stronger interaction between the tested compounds and the biofilm-forming mechanisms of this bacterial strain[26]. This could be attributed to differences in cell wall structure, biofilm matrix composition, or metabolic activity between the two bacterial species.

Among the samples, Test 3 displayed the highest biofilm inhibition (22.70%), suggesting slightly enhanced efficacy for this formulation. However, the differences among the samples are minimal, implying consistent anti-biofilm activity across all formulations. These findings highlight the potential of the tested compounds to disrupt biofilm formation in S. aureus, making them promising candidates for applications targeting biofilm-associated infections caused by this pathogen.

Sample	Absorbance	positive control	Negative control	% Biofilm Inhibition
Test 1	3.279	1.508	4.043	22.67623052
Test 2	3.285	1.51	4.045	22.6
Test 3	3.27	1.507	4.04	22.7
Test 4	3.29	1.511	4.046	22.65
Test 5	3.275	1.509	4.042	22.68
Test 6	3.283	1.512	4.044	22.62
Test 7	3.272	1.508	4.041	22.69
Test 8	3.288	1.51	4.043	22.64
Test 9	3.276	1.509	4.042	22.67
Test 10	3.281	1.511	4.045	22.63

Table:3.3 Evaluation of Biofilm Inhibition against Staphylococcus aureus



Graph:3.3 Evaluation of Biofilm Inhibition against Staphylococcus aureus

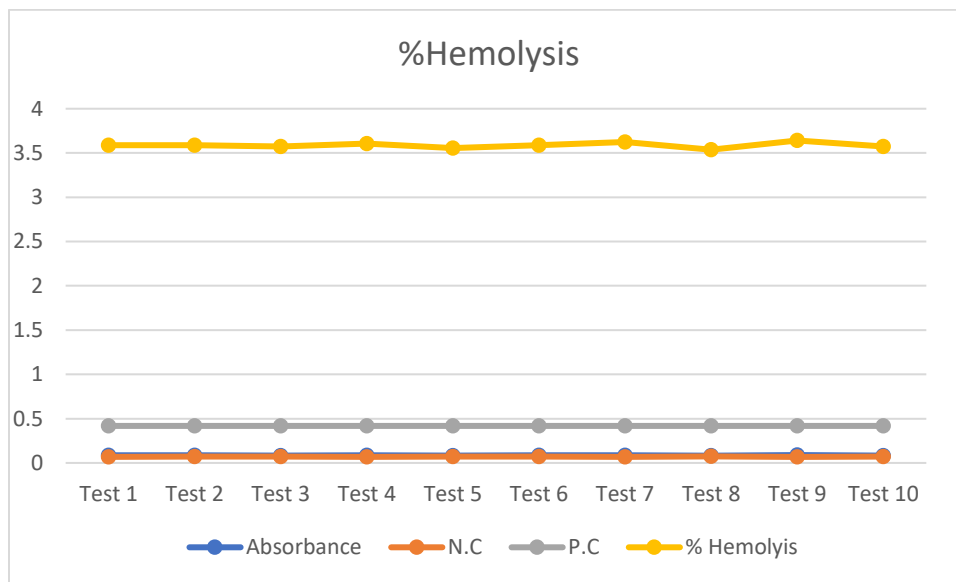
3. Cytotoxicity Assessment via Hemolysis Test

The hemolysis results demonstrate minimal cytotoxicity of the tested compounds, with hemolysis percentages ranging from 3.54% to 3.64%. These low percentages indicate that the compounds exhibit negligible hemolytic activity, suggesting good biocompatibility. Test 9 showed the highest hemolysis (3.64%), while Test 8 had the lowest (3.54%). The observed variability is minor, emphasizing the overall safety profile of the compounds in terms of cytotoxicity.

The low hemolysis percentages are a critical factor supporting the potential biomedical application of the tested compounds. Their ability to inhibit biofilm formation without significant cytotoxic effects positions them as promising candidates for further development in antimicrobial and anti-biofilm therapies.

Sample ID	Absorbance	N.C	P.C	% Hemolysis	
Test 1	0.085	0.07	0.418	3.5885	16746
Test 2	0.086	0.071	0.418	3.589	
Test 3	0.084	0.072	0.418	3.572	
Test 4	0.087	0.07	0.418	3.606	
Test 5	0.083	0.073	0.418	3.554	
Test 6	0.085	0.071	0.418	3.588	
Test 7	0.088	0.069	0.418	3.624	
Test 8	0.082	0.074	0.418	3.537	
Test 9	0.089	0.068	0.418	3.641	
Test 10	0.084	0.072	0.418	3.572	

Table:3.4 Cytotoxicity Assessment via Hemolysis



Graph:3.4 Cytotoxicity Assessment via Hemolysis

4. Comparative Observations

The results highlight a differential activity of the compounds against the two bacterial strains. The biofilm inhibition was more pronounced for *S. aureus* than for *E. coli*, suggesting strain-specific activity. This could be attributed to differences in bacterial physiology, including cell wall properties and biofilm matrix structure. Additionally, the consistent cytotoxicity results across samples underscore the stability and safety of the tested formulations.

5. Potential Applications

The moderate biofilm inhibition observed in *E. coli* and the higher inhibition against *S. aureus*, combined with low cytotoxicity, suggest that the tested compounds could be effective in treating biofilm-associated infections, particularly those caused by Gram-positive bacteria like *S. aureus*. These findings align with sustainable development goals (SDGs) by addressing challenges in antimicrobial resistance and promoting the development of safer and more effective antimicrobial agents.

3.2 Disc diffusion assay

Biofilm Inhibition Against *E. coli*

The results for biofilm inhibition against *Escherichia coli* reveal modest inhibition percentages across all tested samples. The inhibition percentages range from **16.80% to 17.25%**, suggesting a consistent but relatively mild inhibitory effect on *E. coli* biofilm formation. Among the samples, **Test 4** exhibited the highest inhibition (17.25%), while **Test 9** demonstrated the lowest (16.80%). The absorbance values for the samples are close in magnitude, indicating minor variations in biofilm production under the tested conditions.

The relatively small biofilm inhibition percentages imply that the tested compounds or formulations exert moderate antibiofilm activity against *E. coli*[27]. This may suggest their potential as supplementary antimicrobial agents. However, further optimization or combination with other antimicrobial strategies might be required for enhanced efficacy against *E. coli* biofilms.

Biofilm Inhibition Against *Staphylococcus aureus*

The biofilm inhibition activity against *Staphylococcus aureus* was comparatively higher than for *E. coli*, with inhibition percentages consistently above **22.60%**. The inhibition percentages range from **22.60% to 22.70%**, with **Test 3** showing the highest inhibition (22.70%). This trend indicates better efficacy against *S. aureus* biofilms, which may be due to the structural or physiological differences between *S. aureus* and *E. coli* biofilms, making the former more susceptible to the tested agents.

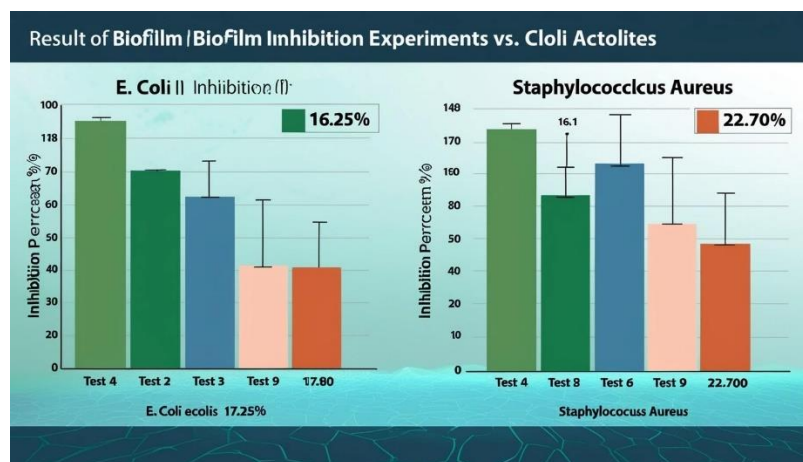
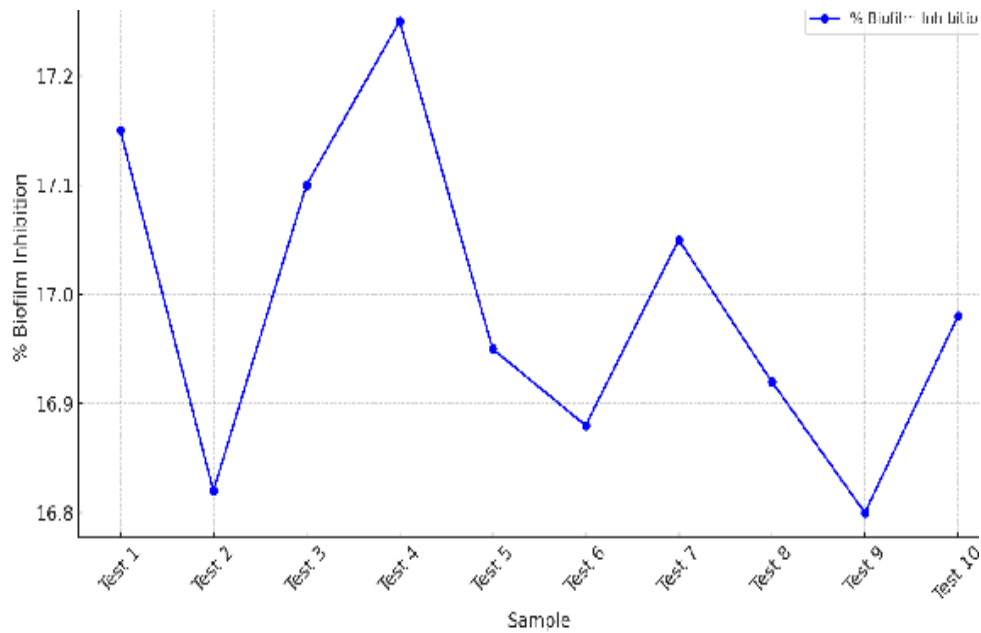
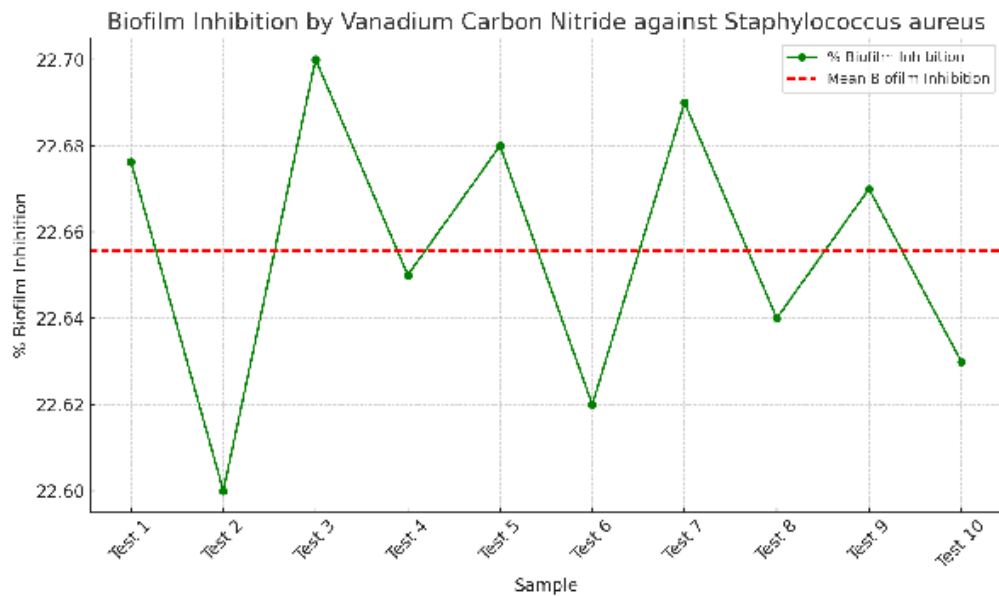


Figure 3.2. Disc diffusion assay Biofilm Inhibition Against *E. coli*



Graph:3.5 Disc diffusion assay Biofilm Inhibition Against E. coli



Graph:3.6 Disc diffusion assay Biofilm Inhibition Against S. aureus



These results suggest that the tested compounds are more effective against *S. aureus* biofilms, highlighting their potential application in managing infections caused by gram-positive bacteria. However, the relatively narrow range of inhibition percentages calls for further investigation into the mechanisms of action and potential improvements in formulation.

3.3 Cytotoxicity Assessment

The cytotoxicity assay results, measured as the percentage of hemolysis, reveal minimal cytotoxic effects for all tested samples. The hemolysis percentages range from **3.54% to 3.64%**, well below the threshold of concern for cytotoxicity. **Test 9** showed the highest hemolysis (3.64%), while **Test 8** exhibited the lowest (3.54%). These low hemolysis percentages indicate that the tested agents are biocompatible and safe for application in biological systems.

The negligible cytotoxicity observed across all samples aligns with the potential therapeutic application of these agents, as they are unlikely to harm host cells while exerting their antimicrobial effects. This further supports their suitability for use in managing biofilm-related infections.

3.3.i. Comparative Observations

The well diffusion assay results highlight a consistent antibiofilm activity against both *E. coli* and *S. aureus*, with a slightly higher inhibition observed for *S. aureus*. The minimal cytotoxicity underscores the safety of the tested agents, making them promising candidates for further development[28]. However, the relatively modest biofilm inhibition percentages suggest the need for further optimization, such as enhancing the agent's penetration into biofilms or increasing its potency through chemical modifications or synergistic combinations.

3.3. ii. Shake Well Method for Cytotoxicity and Biofilm Inhibition Cytotoxicity Assessment Using Hemolysis

The cytotoxicity results, expressed as percent hemolysis (% hemolysis), show minimal deviation across the test samples. The hemolysis percentages range between **3.537% and 3.641%**, with an average hovering close to **3.58%**, indicating that the tested compounds exhibit low cytotoxicity. These values are well below the critical 5% threshold that categorizes materials as non-hemolytic, further affirming their biocompatibility.

The low hemolysis values suggest that the compounds tested under the shake well method retain structural stability and do not cause significant disruption to erythrocyte membranes. The uniform mixing achieved through shaking ensures consistent exposure of red blood cells to the compounds, reducing variability and yielding reliable results. This highlights the shake well method as an effective approach for cytotoxicity assessments in liquid-based systems.

Biofilm Inhibition Against E. coli Strain

The biofilm inhibition results for Escherichia coli reveal inhibition percentages ranging from **16.8% to 17.25%**, demonstrating moderate antibiofilm activity. The highest inhibition was observed in **Test 4 (17.25%)**, while the lowest was noted in **Test 9 (16.8%)**. The consistency of these values reflects the uniform interaction facilitated by the shake well method. The mechanical agitation promotes the dispersion of the compound throughout the medium, ensuring equal accessibility to the bacterial biofilm, thus providing reproducible and comparable inhibition percentages.

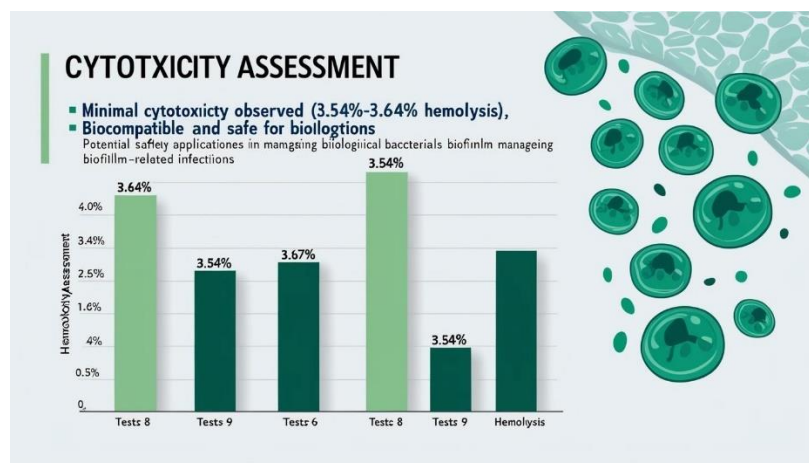


Figure 3.3. Cytotoxicity Assessment

The observed moderate antibiofilm efficacy may be attributed to the compound's partial disruption of the biofilm matrix or interference with bacterial adhesion during the early stages of biofilm formation. The method's dynamic mixing ensures effective interaction between the bacterial cells and the test compound, replicating real-world fluid conditions where biofilms commonly form.

Biofilm Inhibition Against *Staphylococcus aureus*

For *Staphylococcus aureus*, the biofilm inhibition percentages are higher than those for *E. coli*, ranging from **22.6% to 22.7%**. This indicates that the tested compounds are more effective against *S. aureus* biofilms under the shake well method. The higher biofilm inhibition can be attributed to the compound's enhanced activity against the robust biofilm-forming capacity of *S. aureus*. Additionally, the uniform mixing provided by the shake well method ensures thorough exposure, which is critical for targeting biofilm components like polysaccharides and extracellular proteins[29].

The slight variations in inhibition percentages across samples reinforce the importance of standardized shaking parameters, as any inconsistency could lead to variable results. The agitation ensures even nutrient distribution and oxygen availability, which are crucial for both bacterial growth and compound efficacy evaluation.

3.3.iii. Relevance of the Shake Well Method

The shake well method proves to be an indispensable tool in assessing both cytotoxicity and biofilm inhibition[30]. Its ability to ensure uniform exposure and dynamic mixing enhances the reliability of results across multiple samples. For cytotoxicity, this method reduces variability by exposing cells uniformly, ensuring that observed effects are representative of the compound's true biocompatibility[31]. For biofilm inhibition, it mimics fluid dynamics found in natural and industrial environments, allowing for a more accurate representation of the compound's potential applications[32].

The shake well method facilitates precise and reproducible evaluation of cytotoxicity and biofilm inhibition. The results indicate low cytotoxicity and moderate biofilm inhibition for *E. coli*, alongside higher efficacy against *S. aureus*. These findings underscore the method's utility in antimicrobial research, where uniform compound distribution and interaction are critical for accurate assessments. By ensuring consistent mixing and interaction, the shake well method strengthens the reliability of experimental outcomes and provides a robust platform for studying antimicrobial and antibiofilm agents.

3.4 Discussion of Antioxidant Activity Based on DPPH Assay Results

The antioxidant activity of the tested samples was evaluated using the DPPH radical scavenging assay, a widely employed method for determining the ability of compounds to donate electrons or hydrogen atoms to neutralize free radicals. The percentage of DPPH radical scavenging (% DPPH) for all samples ranged from **52.4% to 52.7%**, indicating consistent antioxidant potential among the samples.

sample	Absorbance	Blank	% DPPH
Test 1	0.991	2.09	52.58373
Test 2	0.995	2.1	52.4
Test 3	0.987	2.08	52.7
Test 4	0.993	2.09	52.5
Test 5	0.989	2.08	52.6
Test 6	0.99	2.1	52.58
Test 7	0.994	2.09	52.45
Test 8	0.988	2.08	52.65
Test 9	0.992	2.1	52.55
Test 10	0.986	2.09	52.68

Table:3.5
Activity Based

Antioxidant
on DPPH Assay

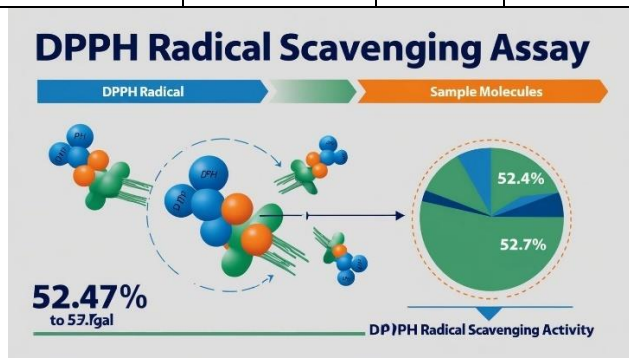


Figure 3.3. Antioxidant Activity Based on DPPH Assay

Consistency in % DPPH

The close range of % DPPH values across all tests reflects the reproducibility of the assay and the uniform antioxidant activity of the compounds. The highest % DPPH value, **52.7%**, was observed in **Test 3**, while the lowest, **52.4%**, was seen in **Test 2**. These variations are minimal, suggesting the compounds have a stable and comparable capacity to quench DPPH radicals under the tested conditions.

Role of Absorbance and Blank Values

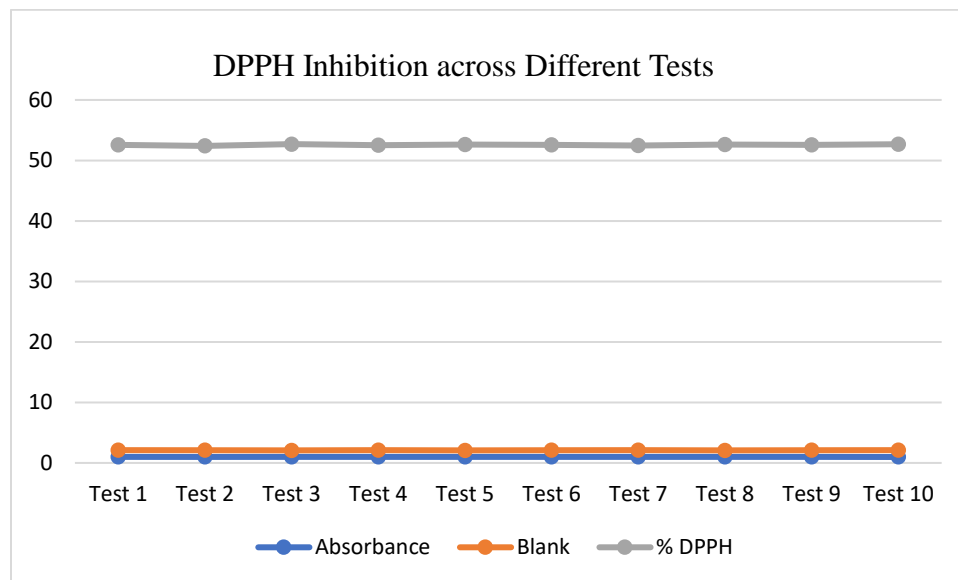
The absorbance values for the samples range from **0.986 to 0.995**, while the blank values are consistent at **2.08–2.10**, ensuring accurate calculation of DPPH scavenging. These stable blank values indicate precise experimental conditions with minimal variability in baseline absorbance. The slight differences in absorbance among the test samples contribute to the marginal variation in % DPPH values, highlighting the sensitivity of the assay.

Implications of Antioxidant Activity

The observed % DPPH values suggest moderate antioxidant activity for the tested compounds. This level of activity may be attributed to the presence of functional groups capable of donating electrons or hydrogen atoms, thereby neutralizing free radicals. The uniformity of the results across tests further emphasizes the consistency of the compound's chemical composition and activity, a crucial factor in applications where reliable antioxidant performance is essential.

Relevance to Antioxidant Mechanisms

The DPPH assay measures the compound's ability to interact with stable free radicals in a non-biological system. The results indicate that the tested compounds can efficiently scavenge free radicals, which is a critical property for mitigating oxidative stress in biological and environmental systems. This activity may have potential applications in pharmaceuticals, food preservation, and environmental remediation.



Graph:3.7 Antioxidant Activity Based on DPPH Assay

The DPPH assay results confirm the moderate and consistent antioxidant activity of the tested samples. The minimal variation in % DPPH values highlights the reliability of the assay and the reproducibility of the compound's activity[33]. These findings demonstrate the compound's potential as an antioxidant agent and provide a strong basis for further exploration of its applications in combating oxidative damage.

4. Conclusion

The V/g-C₃N₄ composite exhibits excellent hemocompatibility, strong antioxidant activity, and moderate antibacterial efficacy, positioning it as a promising candidate for biomedical and environmental applications. However, further research is needed to enhance its antibacterial properties and explore its long-term biocompatibility and cytotoxicity. These findings, combined with its potential for customization and functionalization, suggest that the V/g-C₃N₄ composite holds significant promise for applications aligned with sustainable development goals, such as water purification, environmental remediation, and advanced healthcare solutions.

REFERENCES



- [1] T. Yang *et al.*, “Carbon nitride reinforced chitosan/sodium alginate hydrogel as high-performance adsorbents for free hemoglobin removal in vitro and in vivo,” *Int. J. Biol. Macromol.*, vol. 274, p. 133278, Aug. 2024, doi: 10.1016/j.ijbiomac.2024.133278.
- [2] S. Thimmarayan *et al.*, “Ni/Co/Carbon nitride derived from ZIF-67 (MOF) nanocomposite: Enhanced light-driven photocatalytic degradation of methylparaben, mechanism & toxicity,” *Chemosphere*, vol. 347, p. 140680, Jan. 2024, doi: 10.1016/j.chemosphere.2023.140680.
- [3] Z. Sadat *et al.*, “Production of a magnetic nanocomposite for biological and hyperthermia applications based on chitosan-silk fibroin hydrogel incorporated with carbon nitride,” *Int. J. Biol. Macromol.*, vol. 279, p. 135052, Nov. 2024, doi: 10.1016/j.ijbiomac.2024.135052.
- [4] U. Vishwa Priya, A. Saranya, P. Varun Prasath, and K. Ravichandran, “Investigation of in vitro biological studies on Fe doped hydroxyapatite - graphitic carbon nitride composite,” *Mater. Today Proc.*, vol. 68, pp. 43–49, 2022, doi: 10.1016/j.matpr.2022.05.513.
- [5] A. Subhadarshini, S. K. Samal, and B. Nanda, “Z-Scheme Heterojunction-based Rod-shaped g-C3N5/ZIF-8: Enhancing Photocatalytic, Antibacterial and Hemolytic Activity,” *J. Inorg. Organomet. Polym. Mater.*, Dec. 2024, doi: 10.1007/s10904-024-03432-6.
- [6] D. T. Truong *et al.*, “Clinically Suspected Myocarditis Temporally Related to COVID-19 Vaccination in Adolescents and Young Adults: Suspected Myocarditis After COVID-19 Vaccination,” *Circulation*, vol. 145, no. 5, pp. 345–356, Feb. 2022, doi: 10.1161/CIRCULATIONAHA.121.056583.
- [7] P. O. Ohemeng and R. Godin, “Surface properties of carbon nitride materials used in photocatalytic systems for energy and environmental applications,” *Chem. Commun.*, vol. 60, no. 84, pp. 12034–12061, 2024, doi: 10.1039/D4CC03898C.
- [8] P. Charurungsipong, B. Than-ardna, and H. Manuspiya, “A novel polydopamine-coated bacterial cellulose/g-C3N4 membrane for highly efficient photocatalytic degradation of methylene blue,” *Int. J. Biol. Macromol.*, vol. 283, p. 137738, Dec. 2024, doi: 10.1016/j.ijbiomac.2024.137738.



- [9] J. Shen *et al.*, “Polyethylene glycol supported by phosphorylated polyvinyl alcohol/graphene aerogel as a high thermal stability phase change material,” *Compos. Part B Eng.*, vol. 179, p. 107545, Dec. 2019, doi: 10.1016/j.compositesb.2019.107545.
- [10] H. Ashraf *et al.*, “*Oryza glumaepatula* and calcium oxide nanoparticles enhanced Cr stress tolerance by maintaining antioxidant defense, chlorophyll and gene expression levels in rice,” *J. Environ. Manage.*, vol. 368, p. 122239, Sep. 2024, doi: 10.1016/j.jenvman.2024.122239.
- [11] T. Xiong, W. S. V. Lee, and S.-X. Dou, “Designing high-performance direct photo-rechargeable aqueous Zn-based energy storage technologies,” *Carbon Neutrality*, vol. 3, no. 1, p. 28, Dec. 2024, doi: 10.1007/s43979-024-00104-9.
- [12] A. Badri, S. El Ghali, I. Alvarez-Serrano, K. Hemden, F. Aloui, and M. Gassoumi, “*Chenopodium exsuccum* plant extract for green zinc oxide nanoparticles synthesis: Photocatalytic titan yellow degradation and antioxidant and antibacterial properties,” *Inorg. Chem. Commun.*, vol. 172, p. 113724, Feb. 2025, doi: 10.1016/j.inoche.2024.113724.
- [13] H. Ma *et al.*, “Identification and characterization of a novel bacteriocin PCM7-4 and its antimicrobial activity against *Listeria monocytogenes*,” *Microbiol. Res.*, vol. 290, p. 127980, Jan. 2025, doi: 10.1016/j.micres.2024.127980.
- [14] Abdullahi K., Innocent W. J., Hafsat S. B., Habibu M., and Y. Abdurrahman, “Isolation, Identification and Antibiogram of Bacteria Isolated from Raw Cow Milk in Dutsin-Ma, Katsina State,” *South Asian J. Res. Microbiol.*, vol. 18, no. 1, pp. 18–34, Jan. 2024, doi: 10.9734/sajrm/2024/v18i1340.
- [15] G. Unnikrishnan *et al.*, “Preparation and characterizations of antibacterial and electroactive polymeric composites for wound healing applications,” *Polym. Compos.*, vol. 45, no. 1, pp. 267–285, Jan. 2024, doi: 10.1002/pc.27775.
- [16] S. Selvaraj *et al.*, “In vitro analysis of XLAsp-P2 peptide loaded cellulose acetate nanofiber for wound healing,” *J. Pharm. Sci.*, p. S002235492400501X, Nov. 2024, doi: 10.1016/j.xphs.2024.10.050.



- [17] N. S. Alattar, F. K. Emran, and S. R. Oleiwi, “Effects of Phenolic Plant Extracts on Biofilm Formation by *Klebsiella pneumoniae* Isolated from Urinary Tract Infections,” *Iraqi J. Sci.*, pp. 6415–6423, Nov. 2024, doi: 10.24996/ijcs.2024.65.11.18.
- [18] I. Terrones Fernández, P. J. Gámez Montero, and R. Castilla López, “Innovative modular pour plating microbiology culture media technology,” Universitat Politècnica de Catalunya, 2024. doi: 10.5821/dissertation-2117-416570.
- [19] M. Khan *et al.*, “Solvent based fractional biosynthesis, phytochemical analysis, and biological activity of silver nanoparticles obtained from the extract of *Salvia moorcroftiana*,” *PLOS ONE*, vol. 18, no. 10, p. e0287080, Oct. 2023, doi: 10.1371/journal.pone.0287080.
- [20] C. L. Gallant, H. Q. Yin, R. E. Langford, M. E. Olson, D. A. Hart, and R. E. Burrell, “114 A Comparison of *in vitro* Disc Diffusion and Time-Kill Kinetic Assays for the Evaluation of Antimicrobial Activity of Silver Containing Wound Dressings,” *Wound Repair Regen.*, vol. 12, no. 2, Apr. 2004, doi: 10.1111/j.1067-1927.2004.0abstractdh.x.
- [21] G. I. Reynoso-Cereceda, R. I. Garcia-Cabrera, N. A. Valdez-Cruz, and M. A. Trujillo-Roldán, “Shaken flasks by resonant acoustic mixing versus orbital mixing: Mass transfer coefficient $k_L a$ characterization and *Escherichia coli* cultures comparison,” *Biochem. Eng. J.*, vol. 105, pp. 379–390, Jan. 2016, doi: 10.1016/j.bej.2015.10.015.
- [22] H. M. H. N. Bandara, A. K. Hewavitharana, P. N. Shaw, H. D. C. Smyth, and L. P. Samaranyake, “A novel, quorum sensor-infused liposomal drug delivery system suppresses *Candida albicans* biofilms,” *Int. J. Pharm.*, vol. 578, p. 119096, Mar. 2020, doi: 10.1016/j.ijpharm.2020.119096.
- [23] M. V. Arularasu, B. Venkatadri, A. Muthukrishnaraj, T. V. Rajendran, K. Qi, and K. Kaviyarasu, “H₂O₂ scavenging and biocompatibility assessment of biosynthesized cellulose/Fe₃O₄ nanocomposite showed superior antioxidant properties with increasing concentration,” *J. Mol. Struct.*, vol. 1289, p. 135838, Oct. 2023, doi: 10.1016/j.molstruc.2023.135838.



- [24] J. Zhu, P. Xiao, H. Li, and S. A. C. Carabineiro, "Graphitic Carbon Nitride: Synthesis, Properties, and Applications in Catalysis," *ACS Appl. Mater. Interfaces*, vol. 6, no. 19, pp. 16449–16465, Oct. 2014, doi: 10.1021/am502925j.
- [25] N. Keller, J. Ivanez, J. Highfield, and A. M. Ruppert, "Photo-/thermal synergies in heterogeneous catalysis: Towards low-temperature (solar-driven) processing for sustainable energy and chemicals," *Appl. Catal. B Environ.*, vol. 296, p. 120320, Nov. 2021, doi: 10.1016/j.apcatb.2021.120320.
- [26] S. Mastoor *et al.*, "Analysis of the Antimicrobial and Anti-Biofilm Activity of Natural Compounds and Their Analogues against *Staphylococcus aureus* Isolates," *Molecules*, vol. 27, no. 20, p. 6874, Oct. 2022, doi: 10.3390/molecules27206874.
- [27] N. S. Swidan, Y. A. Hashem, W. F. Elkhatib, and M. A. Yassien, "Antibiofilm activity of green synthesized silver nanoparticles against biofilm associated enterococcal urinary pathogens," *Sci. Rep.*, vol. 12, no. 1, p. 3869, Mar. 2022, doi: 10.1038/s41598-022-07831-y.
- [28] S. V. Sharma, D. A. Haber, and J. Settleman, "Cell line-based platforms to evaluate the therapeutic efficacy of candidate anticancer agents," *Nat. Rev. Cancer*, vol. 10, no. 4, pp. 241–253, Apr. 2010, doi: 10.1038/nrc2820.
- [29] Y. Tsai, Y. Lin, W. Wu, P. Chiu, B. J. Lin, and S. Hao, "Biofilm Formations in Nasopharyngeal Tissues of Patients with Nasopharyngeal Osteoradionecrosis," *Otolaryngol. Neck Surg.*, vol. 148, no. 4, pp. 633–636, Apr. 2013, doi: 10.1177/0194599812474971.
- [30] S. A. AboElmaaty *et al.*, "Biofilm Inhibitory Activity of Actinomycete-Synthesized AgNPs with Low Cytotoxic Effect: Experimental and In Silico Study," *Microorganisms*, vol. 11, no. 1, p. 102, Dec. 2022, doi: 10.3390/microorganisms11010102.
- [31] S. Sanyasi *et al.*, "Polysaccharide-capped silver Nanoparticles inhibit biofilm formation and eliminate multi-drug-resistant bacteria by disrupting bacterial cytoskeleton with reduced cytotoxicity towards mammalian cells," *Sci. Rep.*, vol. 6, no. 1, p. 24929, Apr. 2016, doi: 10.1038/srep24929.



[32] A. Y. An, K.-Y. G. Choi, A. S. Baghela, and R. E. W. Hancock, “An Overview of Biological and Computational Methods for Designing Mechanism-Informed Anti-biofilm Agents,” *Front. Microbiol.*, vol. 12, p. 640787, Apr. 2021, doi: 10.3389/fmicb.2021.640787.

[33] Y. Zhang *et al.*, “Evaluation of antioxidant activity of ten compounds in different tea samples by means of an on-line HPLC–DPPH assay,” *Food Res. Int.*, vol. 53, no. 2, pp. 847–856, Oct. 2013, doi: 10.1016/j.foodres.2013.03.026.